Color Video Denoising by Developing Multiple Transformation Techniques

Ph.D. (Asst. Prof.) Matheel Emaduldeen [*] Rabab Farhan Abass [**]

Abstract

Most of denoising methods have been proposed to perform on still images, while few have been proposed for video denoising and even less when it comes to color sequence. 3-D transform is a good tool for solving a video processing problem such as video denoising because it deals with spatial and temporal correlations between video frames.

This paper aims to propose a methods for video denoising, named “Mixing Sub bands and Double Wiener filter Threshold methods” (MSDWTM). This method are performed with 2-D, 3-D FDWT and it gives a better result compared with the original methods using database of color AVI videos type. When the RMSE equal to (25.0963) it was decreased in 2D and 3-D FDWT method to (7.3511) and (7.1080) RMSE value.

Keywords: video, denoising, wavelet transform.

*Department of computer science/ University of technology
** Department of production engineering and metallurgy/ University of technology

1. Introduction

The last decade has witnessed an overwhelming proliferation of video applications due to the rapid growth of multimedia technology. These video signals are often contaminated by noise during acquisition, storage, and transmission. The presence of noise not only results in unpleasant visual appearance, but also imposes an adverse effect on subsequent video processing tasks, such as video compression, analysis, object tracking, and pattern recognition.Therefore, video denoising is a highly desirable and essential step in video processing systems [1].

The existing video denoising algorithms can be classified into two classes: spatial filtering methods and temporal filtering methods. In spatial methods each frame is filtered individually, ignoring temporal correlations between video frames. This intraframe approach tends to introduce artifacts into the filtered video sequence due to temporal inconsistency. Even the most advanced spatial denoisers, such as Wiener and wavelet filtering, cannot deliver good video denoising results. Therefore, pure spatial denoiser's methods are not appropriate for video. The temporal denoising approach exploits both spatial and temporal correlations [2]. The wavelet transform is a powerful tool to analyze the local information of a signal and obtain a space-frequency description of it [3]. The motivation for using the wavelet transform is that it is good for energy compaction since the small and large coefficients are more likely due to noise and important image features respectively. The small coefficients can be threshold without affecting the significant features of the image. In its most basic form, each coefficient is threshold by comparing against a value, called threshold. If the coefficient is smaller than the threshold, it is set to zero; otherwise it is kept either as it is or modified. The inverse wavelet transform on the resultant image leads to reconstruction of the image with essential characteristics [4].

2. Related Works

In (2005) Nasrat H.A., proposed new algorithms for computing 1-D, 2-D and 3-D wavelet transform [5]. *Bijalwan A.,* and his cluster (2012) proposed threshold estimation method for image denoising in the DWT domain where the algorithm of wavelet threshold is used to calculate the value of threshold. This method is more efficient and adaptive because the parameter required for calculating the threshold based on sub band data [6]. Finally *Bahich M.,* and his cluster (2013) proposed a comparative study of one and two-dimensional wavelet-based techniques for noisy fringe patterns analysis [3].

3. Wiener Filter

Filters play a major role in the image restoration process. There are two general motivations for filtering. One is to improve the quality of the inputs; the other is to process or extract information from the input data. There are two types of filters that are used to eliminate the amount of noises depending on the time or frequency criteria, these are spatial filters and frequency filters [7].

Frequency domain filtering operates by using the Fourier transform representation of images. This representation consists of information about the spatial frequency content of the image, also referred to as the spectrum of the image. Wiener filter is one of the frequency domain filters [3].

The Wiener filter, also called a minimum mean square estimator (developed by Norbet Wiener in 1942), alleviates some of the difficulties inherent in another filters by attempting to model the error in the restored image through the use of statistical methods. After the error is modeled, the average error is mathematically minimized, thus the term *minimum mean square estimator* was proposed. The resulting equation is the Wiener filter [7].

$$R_W(u,v) = \frac{H^*(u,v)}{\left|H(u,v)\right|^2 + \left[\dfrac{S_n(u,v)}{S_I(u,v)}\right]} \quad (1)$$

where: $H^*(u,v)$ is the complex conjugate of $H(u,v)$.

$S_I(u,v) = |I(u,v)|^2$ is the power spectrum of the original image.

$S_n(u,v) = |N(u,v)|^2$ is the power spectrum of the noise.

This equation assumes a square image of size $N \times N$. The complex conjugate can be found by negating the imaginary part of a complex number. If we assume that the noise term $Sn(u,v)$ is zero, this equation reduces to an inverse filter since $|H(u,v)|^2 = H^*(u,v)H(u,v)$, as the contribution of the noise increases, the filter gain decreases [7].

This seems reasonable, in portions of the spectrum uncontaminated by noise we have an inverse filter, whereas in portions of the spectrum heavily corrupted by noise, the filter attenuates the signal, with the amount of attenuation being determined by the ratio of the noise spectrum to the uncorrupted image spectrum.

The Wiener filter is applied by multiplying it by the Fourier transform of the degraded image, and the restored image is obtained by taking the inverse Fourier transform of the result, as follows[7]:

$$\hat{I}(r,c) = \mathrm{F}^{-1}[\hat{I}(u,v)] = \mathrm{F}^{-1}[\mathrm{R}_{\mathrm{W}}(u,v)\,\mathrm{D}(u,v)] \quad (2)$$

4. Discrete Wavelet Transform

In DWT there are two sets of functions, called scaling functions and wavelet functions, which are associated with low pass and high pass filters, respectively [8]. The low pass filter (LPF) is determined from the scaling function, and the high pass filter (HPF) is determined from both the wavelet and scaling functions [9]. The wavelet and scaling functions are respectively given as in equations (3) and (4):

$$\varphi(t) = \sum_k h(k)\sqrt{2}\varphi(2t-k) \quad (3)$$

$$\psi(t) = \sum_k g(k)\sqrt{2}\varphi(2t-k) \quad (4)$$

Where h(k), g(k) are the scaling function coefficients and wavelet function coefficients respectively[10] .The traditional wavelet denoising is usually each frame denoising, without considering the correlation between each frame movement, moving objects trailing phenomenon. A new video denoising algorithm is the video signal as a special 3-D signal, three-dimensional transform to regard it as a whole, the algorithm is effective to solve the moving object trailing, flashing and algorithm robustness problems [11].

The 3-D DWT is like a 1-D DWT in three directions. First, the process transforms the data in the x-direction. Next, the low and high pass outputs both feed to other filter pairs, which transform the data in the y-direction. These four output streams go to four more filter pairs, performing the final transform in the z-direction. The process results in 8 data streams. Applying one level of 3-D DWT is the process of transforming the original volume into 8 octants in its wavelet domain. Mathematically, 3-D DWT is the process of applying 1-D DWT on each vector in Z-axis which has the same X-axis and Y-axis coordinates after applying 2-D DWT for all comprising frames [12].

5. Denoising Concepts

Since images and video signals are often corrupted by different types of noise during acquisition and transmission. Denoising of color images and video signals is highly desirable in order to enhance the overall perceptual quality, increase compression effectiveness, facilitate transmission bandwidth reduction, and facilitate accuracy in processes like feature extraction and pattern recognition that might be involved[11]. So

wavelet analysis has been demonstrated to be one of the powerful methods for performing image noise reduction [12].

The procedure for noise reduction is applied on the wavelet coefficients obtained after applying the wavelet transform to the image at different scales. The motivation for using the wavelet transform is that it is good for energy compaction since the small and large coefficients are more likely due to noise and important image features respectively. The small coefficients can be threshold without affecting the significant features of the image. In its most basic form, each coefficient is threshold by comparing against a value, called threshold. If the coefficient is smaller than the threshold, it is set to zero; otherwise it is kept either as it is or modified. The inverse wavelet transform on the resultant image leads to the reconstruction of the image with essential characteristics [13].

6. Thresholding Types

Thresholding is one of the most commonly wavelet signal processing tools. It is widely used in noise reduction, signal and image compression or recognition [13].

6.1 Hard Threshold

Hard Thresholding is also called "kill / keep" strategy [14] or "gating" [13]. If the signal or a coefficient value is below a present value it is set to zero, that is [13]:

$$\hat{X}_k^j = T_h\,(G_k^j, Thv) = \begin{cases} G_k^j, & |\,G_k^j\,| > Thv\,; \\ 0, & |\,G_k^j\,| \le Thv\,. \end{cases} \qquad (5)$$

where Thv is the threshold value or the gate value.

Hard thresholding can be described as the usual process of setting to zero the wavelet coefficients whose absolute values are less than or equal to the threshold value Thv.

6.2 Soft Threshold

Soft thresholding is an alternative scheme of hard thresholding and can be stated as[14]:

$$\hat{X}_k^j = T_s(G_k^j, Thv) = \begin{cases} sign(G_k^j) * (|G_k^j| - Thv), & |G_k^j| > Thv \\ 0, & |G_k^j| \le Thv \end{cases} \quad (6)$$

Where :

$$sign(G_k^j) = \begin{cases} +1, & if\ G_k^j > 0; \\ 0, & \text{if } G_k^j = 0; \\ -1 & if\ G_k^j < 0. \end{cases}$$

Soft thresholding is an extension of hard thresholding, firstly setting to zero the wavelet coefficients whose absolute value are less than or equal to *Thv*, then shrinking the non zero coefficients towards zero by a threshold value *Thv*[14].

6.3 Semisoft Threshold

Bruce and Gao showed that hard thresholding would cause a bigger variance, while soft thresholding will tend to have a bigger bias because all larger coefficients are reduced by Thv. To prevent the drawback of hard and soft thresholding, they proposed a semi-soft thresholding approach as given in the following equation [15]:

$$\hat{X}_k^j = T_{semi\_soft}(G_k^j, Thv) = \begin{cases} 0 & if \left|G_k^j\right| \le Thv \\ sign\{G_k^j\}\dfrac{\overline{Thv}(\left|G_k^j\right| - Thv)}{\overline{Thv} - Thv} & \text{if } Thv < \left|G_k^j\right| \le \overline{Thv} \\ G_k^j & if \mid G_k^j \mid > \overline{Thv} \end{cases} \quad (7)$$

The aim of semi-soft is to offer a compromise between hard and soft thresholding by changing the gradient of the slope. This scheme requires two thresholds, a lower threshold Thv and an upper threshold $\overline{Thv}$, where $\overline{Thv}$ is estimated to be twice the value of lower threshold Thv. There is no attenuation for inputs beyond $\pm Thv$. For inputs below or equal to $\pm Thv$, the output is forced to zero. For inputs that lie between $\pm Thv$ and $\pm \overline{Thv}$ the output depends on the gradient formula [15]:

$$sign\{G_k^j\}\frac{\overline{Thv}(\left|G_k^j\right| - Thv)}{\overline{Thv} - Thv} \quad (8)$$

7. Performance Measurements

For visual images corrupted by a certain type of noise, optimal noise removal does not have a simple quantitative measure, since a filtered image with distracting artifacts may still result in a relatively small Mean Square Error (MSE). Thus, overall visual quality must also be examined. For each of the implemented algorithm, visual evaluation of filter performance will be made with respect to noise attenuation, detail and edge preservation (test subjects). Although MSE is also listed for each processed image, the MSE values should generally serve as secondary indicator of the filter performance [4].

The commonly used objective measures are the MSE, the Signal-to-Noise-Ratio (SNR), and the Peak-Signal-to-Noise-Ratio (PSNR). We can define the error between an original, and denoised (reconstructed) pixel values as [4]:

$$\text{error}(r,c) = x(r,c) - \hat{x}(r,c) \tag{9}$$

where: *x(r,c)* is the original image and $\hat{x}(r,c)$ is a reconstructed image.

Next, we can define the total error between the original and denoised image of size $(M * N)$ as [4]:

$$Total\ \ error = \sum_{r=0}^{M-1} \sum_{c=0}^{N-1} [x(r,c) - \hat{x}(r,c)] \tag{10}$$

The MSE is found by taking the sum of the squared errors divided by the total number of pixels in the image "mean" as follows:

$$\text{MSE} = \frac{1}{M * N} \sum_{r=0}^{M-1} \sum_{c=0}^{N-1} [x(r,c) - \hat{x}(r,c)]^2 = \frac{NORM[x(r,c) - \hat{x}(r,c)]}{M * N} \tag{11}$$

So, the Root Mean Square Error (RMSE) is as follows [4]:

$$RMSE = sqrt(SNR) = sqrt\left(\frac{NORM[x(r,c) - \hat{x}(r,c)]}{M * N} \right) \tag{12}$$

The smaller the value of the error metrics, the better the denoised image represents the original image. Alternatively, with the SNR metrics, a large number implies a better image. The SNR metrics considers the denoised image $\hat{x}(r,c)$ to be the "signal", and the error to be the "noise". So, SNR can be defined as [13]:

$$\mathrm{SNR} = 10\log_{10}\left(\frac{\sum_{r=0}^{M-1}\sum_{c=0}^{N-1}[\hat{x}(r,c)]^2}{\sum_{r=0}^{M-1}\sum_{c=0}^{N-1}[x(r,c)-\hat{x}(r,c)]^2}\right) = 10\log_{10}\left(\frac{\mathrm{NORM}(\hat{x}(r,c)}{\mathrm{NORM}[x(r,c)-\hat{x}(r,c)]}\right) \quad (13)$$

Another popular error measurement is the PSNR. It is based upon the sum of the squared differences between corresponding pixels of the reconstructed image and the reference (original) image. The exact formula is given below [13]:

$$\mathrm{PSNR} = 10\log_{10}\left(\frac{[\max(original\ \ image)-\min(original\ \ image)]^2}{\frac{1}{M*N}\sum_{r=0}^{M-1}\sum_{c=0}^{N-1}[x(r,c)-\hat{x}(r,c)]^2}\right) \quad (14)$$

8. The Proposed Method

Transformation techniques are good solutions for image and video denoising problems. A new mixing sub bands and threshold methods to denoise a noisy video with Additive Gaussian White Noise type was proposed. This method named *"Mixing Sub bands and Double Wiener filter Thresholding Methods"* (MSDWTM) is applied first with (2-D FDWT) and (3-D FDWT).

Wiener filter is suitable filter for denoising process and it is worked as *global wiener filter* which is applied over the whole image and it behaves very poorly in the presence of large noise. *Local wiener filter* is applied on small block of image at a time and it behaves good in the presence of large noise and the edges are well handled by it.

A video denoising based on 2-D, 3-D FDWT consists of different stages, these are:

1. **Frames conversions:** this is the first stage, the digital video which is type of AVI color video entered to the system. This video sequence is converted in this block to process each one as a frame.

2. Adding Additive Gaussian White noise type: after the process of converting the digital video to frames is completed, the next step is adding the Gaussian white noise type to these frames.

3. Applying decomposition: the noisy frame is converted from time domain to frequency domain using one of the transformation types (2-D FDWT, 3-D FDWT). In 2-D FDWT the decomposition process has been applied on each frame alone, which produced four sub bands:
low frequency content (LL), and high frequency contents (LH, HL and HH). In 3-D FDWT, the decomposition process has been applied on the consecutive frames, which produced eight sub bands: low frequency contents (LLL), high frequency contents (LLH,LHL,LHH,HLL,HLH,HHL and HHH).

4. Apply thresholding methods: three types of thresholding methods which are (Hard, Soft and Semisoft) have been applied on it.

5. Applying reconstruction: after applying the thresholding methods, the inverse transform has been applied to return the signal from the frequency domain to time domain.

6. Denoised frames: the inverse process produces the denoised frames, these frames then must be tested by the fidelity criteria such as RMSE, SNR and PSNR measurements.

The algorithm of 2-D FDWT decomposition is shown in Figure (1):

Input: Frames sequence, transformation filter matrix.
Output: M frames, each frame contain four sub bands LL, HL, LH and HH.
Step 1: Input one noisy frame at a time.

Step 2: Apply row transformation by multiplying the transformation filter matrix with the R band matrix.
Step 3: Apply column transformation by transposing the resulting matrix from step3 and multiplying the transformation filter matrix with it.
Step 4: The four sub bands can be obtained after transposing the resulting matrix from step 4.
Step 5: Repeat the above three steps on the (G, B) bands then, connect the decomposed three bands to produce the decomposed frame.
Step 6: If there are another noisy frames then, go to step 2.

Figure (1): The algorithm of 2-D FDWT decomposition.

The algorithm of 3-D FDWT decomposition are shown in Figure (2):

Input: Frames sequence, transformation filter matrices.
Output: M frames, each frame contains eight sub bands LLL, HLL, LLH, HLH, LHL, HHL, LHH and HHH.
Step 1: Input M noisy frames.
Step 2: Apply 2-D FDWT decomposition on to each band (R, G, and B) and on each frame in M frames.
Step 3. Apply 1-D FDWT algorithm to each (N*N) elements in all M matrices in Z-direction for R band as shown bellows:
For each *i,j* construct the Mx1 input vector.
Construct an MxM filter transformation matrix.
Multiply filter transformation matrix with the matrix resulting from step (4).
Step 4: Repeat step 4 for G and B bands.
Step 5: For all three bands (R,G and B), collect each frame bands to get M decomposed frames with eight sub bands.
Step 6: If there are another noisy frames then, go to step 2.

Figure (2): The algorithm of 3-D FDWT decomposition.

The algorithm of one level 2-D FDWT reconstruction are illustrated in Figure (3).

Input: M frames after the decomposition step, and each frame contains four sub bands LL, HL, LH and HH, inverse transformation filter matrix.

Output: Reconstructed M frames.

Step 1: Input one decomposed frame at a time.

Step 2: Apply column transformation by multiplying the inverse transformation filter matrix with the R band transposed matrix.

Step 3: Apply row transformation by transposing the resulting matrix from step 3 and multiplying the inverse transformation filter matrix with it.

Step 4: Repeat the above two steps on the (G, B) bands, then connect the reconstructed three bands to produce the reconstructed frame.

Step 5: If there are another decomposed frames, then go to step 2.

Figure (3): The algorithm of one level 2-D FDWT reconstruction.

Input: M frames after the decomposition step, and each frame contains eight sub bands LLL, HLL, LLH, HLH, LHL, HHL, LHH and HHH, inverse transformation filter matrices.
Output: Reconstructed M frames.
Step 1: Input M decomposed frames.
Step 2: Apply 1-D IFDWT algorithm to each (N*N) elements in all M frames in Z-direction for R band:
For each *i,j* construct the Mx1 input vector.
Construct an MxM filter transformation matrix.
Multiply transformation inverse filter matrix with the matrix resulting from step (3).
Step 3: Repeat step 3 for G and B bands.
Step 4: Apply 2-D IFDWT to each frame in M frames.
Step 5: Collect each frame bands to get M reconstructed frames.
Step 6: If there are another decomposed frames, then go to step 2.

Figure (4): The algorithm of 3-D IFDWT.

The general block diagram of video denoising using 2-D MSDWTM is illustrated in figure (5),where the digital video will be converted to frames ,adding Gaussian white noise then perform the proposed 2-D MSDWTM, the final step is to test the denoised frame according to RMSE,SNR and PSNR measurement .

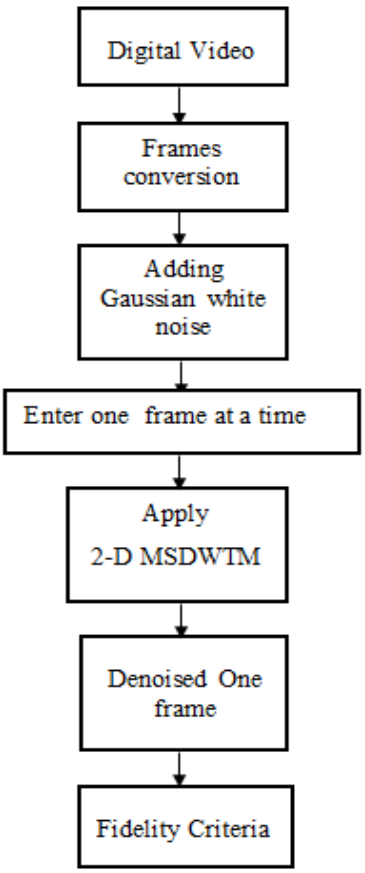

Figure 5: main block diagram of video denoising using 2-D MSDWTM.

The general framework of 2-D MSDWTM with 2-D FDWT is illustrated in Figure (6).

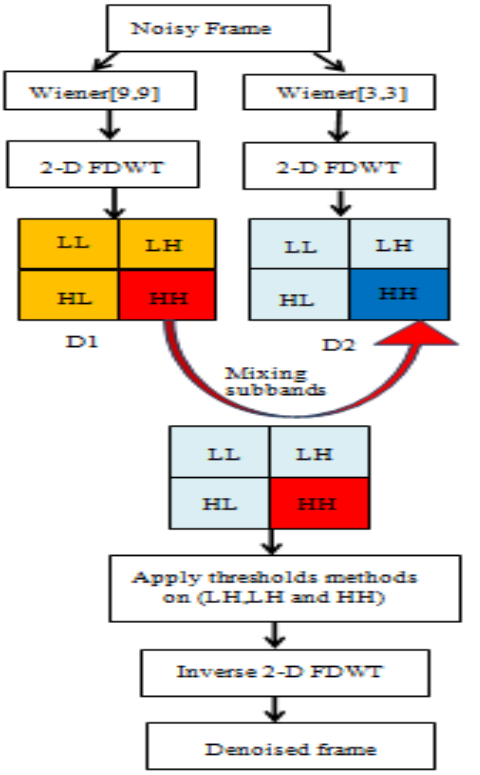

Figure 6: The framework of 2-D MSDWTM

The algorithm is stated bellow in Figure (7):

Input: Noisy frames sequence.
Output: Denoised frames.
Step 1: Input one noisy frame at a time.
Step 2: Denoised it using double local wiener filter 3× 3 and 9× 9 kernel.
Step 3: Apply 2-D FDWT decomposition on each of them to introduce four sub bands of each of them (LL, LH, HL and HH).
Step 4: Perform mixing sub band (replace HH sub band from D2 with HH from D1).
Step 5: Apply the threshold methods on the detail sub bands (LH, HL and HH).
Step 6: Perform inverse 2-D FDWT to produce the denoised frame.
Step 7: If there are another noisy frames, then go to step 2.

Figure (7): The algorithm of 2-D MSDWTM

The general block diagram of video denoising using 3-D MSDWTM is explained in figure (8),where the digital video will be converted to frames ,adding Gaussian white noise then perform the proposed 3-D MSDWTM (which will be explained in detail in figure (9)) , the final step is to test the denoised frames according to RMSE,SNR and PSNR measurement .

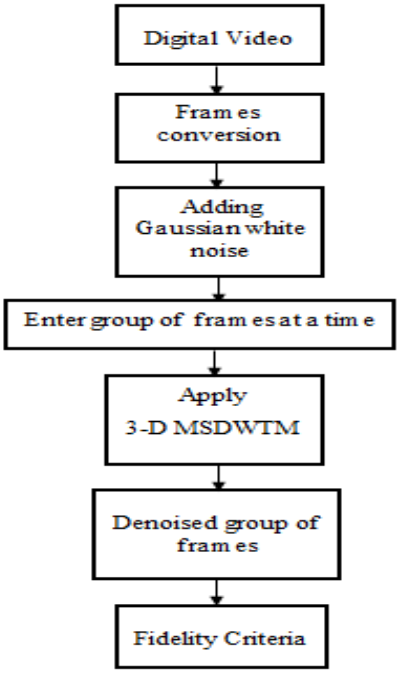

Figure 8: main block diagram of video denoising using 3-D MSDWTM

The general framework of 3-D MSDWTM is illustrated in Figure (9).

9. Results

The threshold that produces the minimum RMSE is the optimal one. Figure (11) produces the RMSE versus threshold values that are plotted of noisy 20th frame and denoised using 2-D FDWT with hard thresholding. Note that, the optimal threshold value has equal to (43) which gives the minimum RMSE.

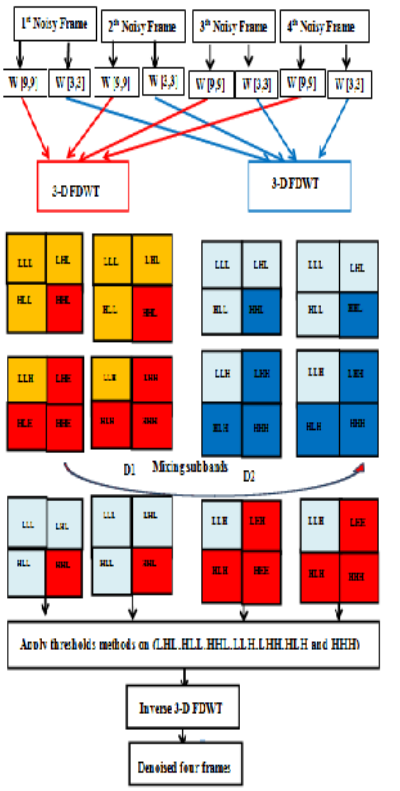

Figure 9: The framework of 3-D MSDWTM

The algorithm is stated bellow in Figure (10):

Input: Noisy frames sequence.
Output: Denoised frames.
Step 1: Input four noisy frames at a time.
Step 2: Denoised them using double local wiener filter 3× 3 and 9× 9 kernel for each of them.
Step 3: Apply 3-D FDWT decomposition to introduce two groups of eight sub bands (LLL, LHL, HLL, HHL, LLH, LHH, HLH and HHH).
Step 4: Perform mixing sub bands (replace HHL, LHH, HLH and HHH sub band from D2 with HHL, LHH, HLH and HHH from D1).
Step 5: Apply the threshold methods on the sub bands (LHL, HLL, HHL, LLH, LHH, HLH and HHH).
Step 6: Perform inverse 3-D FDWT to produce the denoised four frames.
Step 7: If there are another noisy frames, then go to step 2.

Figure (10): Algorithm of 3-D MSDWTM.

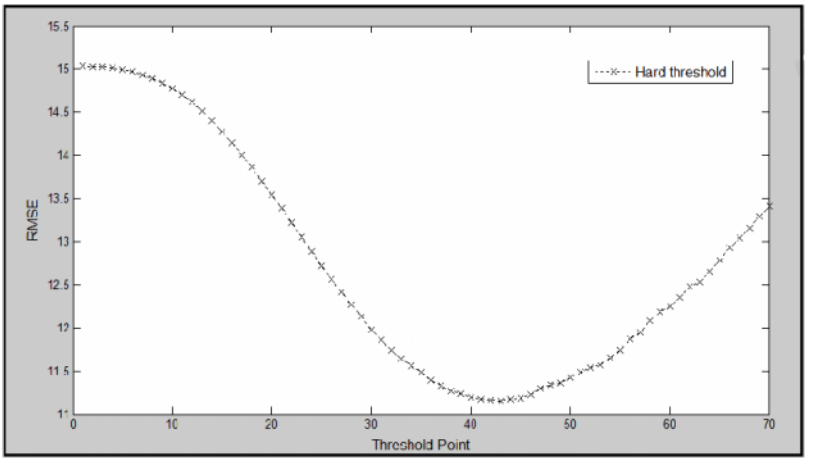

Figure (11): RMSE versus threshold plot obtained by adding Gaussian white noise with σ =15 using 2-D FDWT.

As one can see in figure (12), the RMSE versus threshold values are plotted of 2-D FDWT with Haar filter using hard, soft and semisoft

thresholds methods with optimal thresholds values (Th=43, Ts=10 and Tse= 30) respectively and the thresholds are applied on whole of decomposed frame. Note that, the minimum RMSE can be obtained using semisoft threshold.

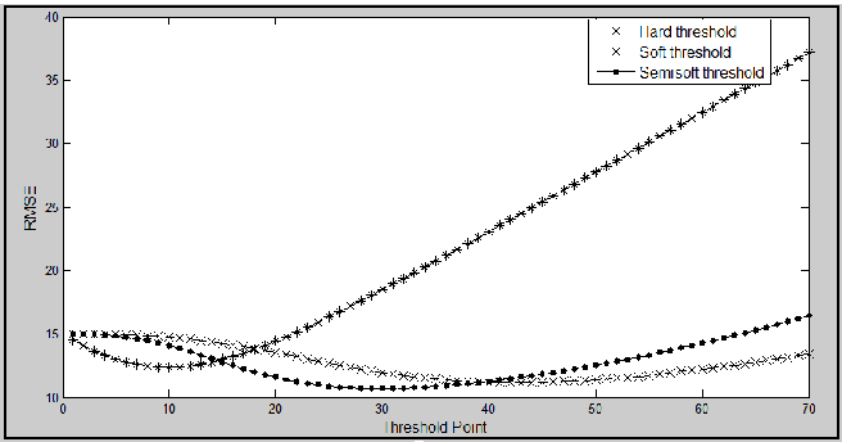

Figure (12): RMSE versus threshold plot obtained by adding Gaussian white noise with σ =15 using 2-D FDWT using different thresholds types.

Table (1) describes the RMSE and SNR of a 20th frame of '*Xylophone*' AVI color video using different noise level (σ) and different thresholds types with DB4 filter. It is clear that semisoft threshold gives a better result than hard and soft threshold.

The objective measures of 2-D FDWT with semisoft thresholding scheme with optimal thresholds values is compared in table (2) that describes the RMSE, SNR and PSNR of different color AVI videos types *('Xylophone', 'Mosaicking' ,'Scenevideoclip', 'Shuttle','Visionface','Traffic', 'Train' ,'Warnsigns' and 'Vipmen'* respectively *)* of the noisy 35th frame (σ=20).

Table (1): RMSE, SNR using 2-D FDWT in Hard thresholding (HT), Soft thresholding (ST) and Semisoft thresholding (SET).

	Noisy frame		Denoising by 2-D FDWT thresholding						Optimal threshold		
			HT	ST	SET	HT	ST	SET			
σ	RMSE	SNR dB	RMSE	RMSE	RMSE	SNR dB	SNR dB	SNR dB	T_h	T_s	T_{se}
5	5.0193	28.0066	4.5030	4.4353	**4.2355**	28.9444	28.9791	**29.4753**	12	3	9
10	10.0385	22.0092	7.6990	8.3812	**7.3482**	24.2926	23.3680	**24.6953**	27	6	20
15	15.0578	18.5241	10.8907	12.2522	**10.4904**	21.2889	19.9699	**21.6115**	43	10	30
20	20.0770	16.0752	14.2829	16.0876	**13.7209**	18.9483	17.5173	**19.2900**	54	14	39
25	25.0963	14.1995	17.9089	19.8730	**17.0908**	17.0021	15.6044	**17.3957**	67	18	47

Table (2): RMSE, SNR and PSNR results with Haar filter using 2-D FDWT.

Noisy frames				Denoising by 2-D FDWT and Semisoft thresholding			
Video name	RMSE	SNR dB	PSNR dB	RMSE	SNR dB	PSNR dB	Optimal threshold
Xylophone	20.0276	16.0530	21.6096	13.9202	19.1421	24.7916	39
Mosaicking	19.9967	17.7307	21.0426	13.6000	21.0520	24.4283	41
Scenevideoclip	20.0535	20.0473	22.0768	17.5962	21.1609	23.2226	31
Shuttle	20.0770	18.3833	21.3812	12.2643	22.6117	25.6635	49
Visionface	20.0770	16.0849	22.0426	14.6939	18.7054	24.7553	35
Traffic	20.0283	16.4983	21.3160	14.0120	19.5370	24.4409	41
Train	19.9593	15.9440	21.2887	15.1867	18.2759	23.7134	35
Warnsigns	19.9632	17.6894	21.0121	13.0600	21.3612	24.7489	46
Vipmen	20.0818	15.7665	22.0197	13.1721	19.3283	25.6887	40

Figure (13) shows 35th frame from the above different AVI color videos with noise level σ=20 and with 2-D FDWT and DB4 filter with semisoft thresholding.

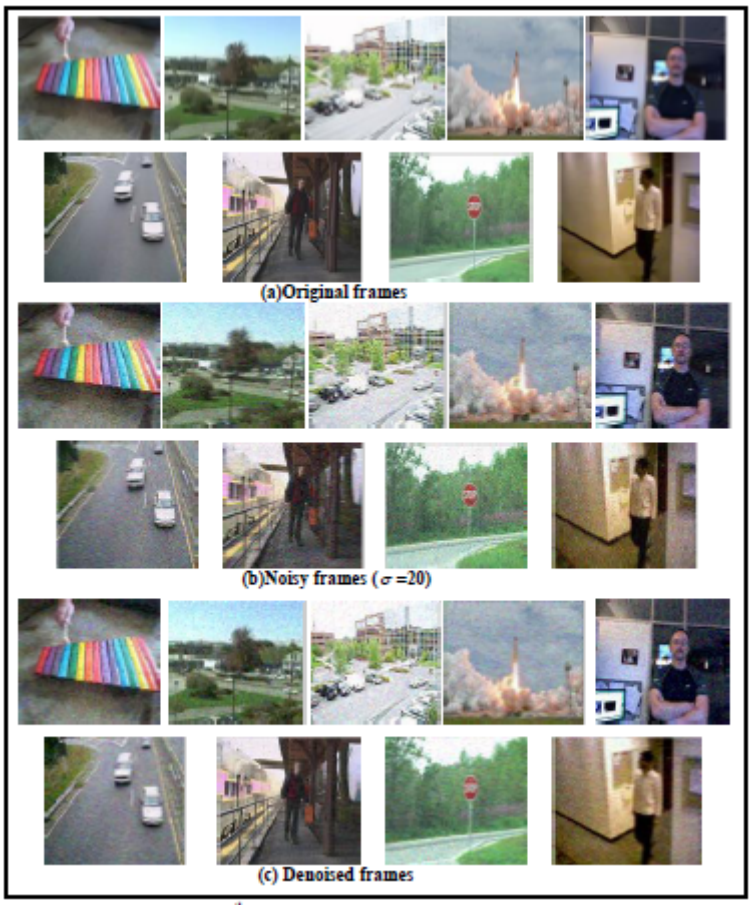

Figure (13) :The 35th frame from the above different AVI color videos with noise level σ=20.

Table (3) shows the results of removing the noise from the noisy 35th frame from each of '*Shuttle'* and '*Vipmen'* AVI video type with different noise levels and with different filter types (*Haar, DB4, DB6* and *DB8*). In the first video *'Shuttle'*, when the noise level is equal to (5), the

PSNR of DB6 is equal to (35.7923) which is the optimal result. For noise levels (10, 15, 20 and 25), the PSNR of DB8 are equal to (30.9867), (28.1709), (26.0753) and (24.3693) respectively which are the optimal results. In the second video *'Vipmen'*, when the noise levels (5, 10, 15 and 20), the PSNR of DB6 are equal to (36.2265), (31.3166), (28.3808) and (26.1207) respectively which are the optimal results. When the noise level is equal to (25) the PSNR of DB8 equal to (24.2658) which is the optimal result. In general, all Daubechies filters (DB4, DB6 and DB8) are given the best result compared with Haar filter.

Table (3): PSNR denoising results of two AVI video with different types of 2-D FDWT filters and with different noise levels.

Shuttle									
σ	**Noisy frame PSNR**	**Haar PSNR**	**T**	**DB4 PSNR**	**T**	**DB6 PSNR**	**T**	**DB8 PSNR**	**T**
5	33.4224	35.3870	9	35.7287	10	**35.7923**	9	35.7783	9
10	27.4018	30.4856	20	30.8106	21	30.9646	22	**30.9867**	22
15	23.8799	27.6392	34	27.9802	36	28.1652	36	**28.1709**	36
20	21.3812	25.6635	49	25.9369	49	26.0675	50	**26.0753**	50
25	19.4430	24.0736	63	24.2552	62	24.3478	62	**24.3693**	62
Vipmen									
σ	**Noisy frame PSNR**	**Haar PSNR**	**T**	**DB4 PSNR**	**T**	**DB6 PSNR**	**T**	**DB8 PSNR**	**T**
5	34.0609	35.9889	9	36.1999	9	**36.2265**	9	36.1745	9
10	28.0403	30.9719	20	31.1821	20	**31.3166**	21	31.2303	20
15	24.5184	27.9644	30	28.2429	31	**28.3808**	32	28.3244	32
20	22.0197	25.6887	40	26.0029	41	**26.1207**	42	26.1029	42
25	20.0815	23.8706	50	24.1537	51	24.2490	51	**24.2658**	51

Table (4) shows the results of eliminating the noise from 40th frame of two AVI video (*'Shuttle'* and *'Traffic'* **)** and comparing those results with different decomposition of 2-D FDWT levels. From this table, the most

decomposition level two gives the best RMSE over the other levels in the two cases.

In the implementation of 3-D FDWT, the consecutive noisy frames (noisy 3-D signal) are performed at a same time depending on the length of the filter that is used in the transformation process. For each of Haar and DB4 filter here, four consecutive noisy frames are transformed at the same time. For each of DB6 and DB8 eight consecutive noisy frames are transformed at the same time.

As one see in figure (14), the RMSE versus of threshold values are plotted of 3-D FDWT with Haar filter using hard, soft and semisoft thresholds methods, with optimal thresholds values (Th=48, Ts=14 and Tse= 34) respectively and the thresholds are applied on the whole of decomposed frame. Note that, the minimum RMSE can be obtained using semisoft threshold.

Table (4): RMSE denoising results with two AVI video and different noise levels of 2-D FDWT in different decomposition levels.

Video name		Filtered Frame in the 2-D FDWT domain							
Shuttle		L=1		L=2		L=3		L=4	
σ	RMSE	RMSE	T	RMSE	T	RMSE	T	RMSE	T
5	5.0193	3.8500	10	**3.7817**	9	3.8187	9	3.8274	9
10	10.0385	6.8129	21	**6.3845**	20	6.4416	19	6.4833	19
15	15.0578	9.4170	35	**8.4462**	33	8.5530	31	8.6681	30
20	20.0770	11.9115	50	**10.0398**	47	10.1750	45	10.3372	44
25	25.0963	14.4553	62	**11.3877**	62	11.4219	59	11.6630	57
Video name		Filtered Frame in the 2-D FDWT domain							
Traffic		L=1		L=2		L=3		L=4	
σ	RMSE	RMSE	T	RMSE	T	RMSE	T	RMSE	T
5	5.0193	**4.2700**	8	4.2738	7	4.2853	7	4.2885	7
10	10.0385	7.7232	18	**7.441**	17	7.4611	17	7.4809	17
15	15.0578	10.9497	28	**10.1742**	27	10.198	26	10.1886	27
20	20.0770	14.0765	38	**12.5227**	39	12.5279	37	12.5466	38
25	25.0963	17.1559	48	14.5227	51	**14.4041**	52	14.5043	50

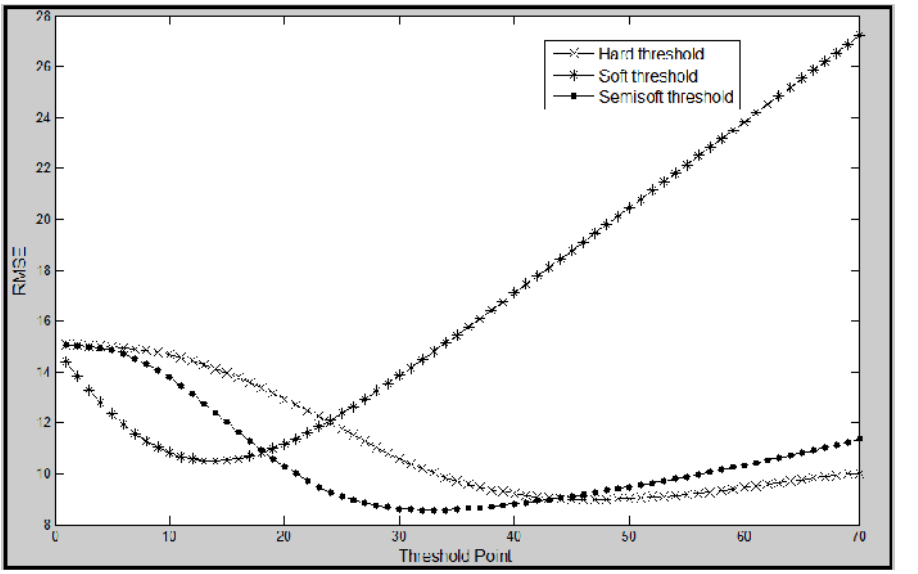

Figure (14): RMSE versus threshold plot obtained by adding Gaussian white noise with σ =15 using 3-D FDWT with different threshold types.

Table (5) describes the RMSE and SNR of the 20th frame of '*Xylophone*' AVI color video using different noise levels (σ) and different thresholds types and with DB4 filter. It is clear that semisoft threshold gives a best result than hard and soft threshold.

Table (5): RMSE, SNR using 3-D FDWT in Hard Threshold (HT) , Soft Threshold (ST) and Semisoft Threshold (SET).

	Noisy frame		Denoising by 3-D FDWT thresholding						Optimal threshold		
			HT	ST	SET	HT	ST	SET			
σ	RMSE	SNR dB	RMSE	RMSE	RMSE	SNR dB	SNR dB	SNR dB	T_h	T_s	T_{se}
5	5.0193	28.0066	3.5663	3.7184	**3.3364**	30.9656	30.5117	**31.5454**	14	4	11
10	10.0385	22.0092	5.6128	6.7695	**5.3574**	27.0303	25.1992	**27.4337**	31	9	22
15	15.0578	18.5241	7.5202	9.7394	**7.1991**	24.4925	21.9328	**24.8700**	47	15	34
20	20.0770	16.0752	9.4382	12.6645	**9.0893**	22.5211	19.5408	**22.8456**	62	20	45
25	25.0963	14.1995	11.4324	15.5733	**11.0397**	20.8565	17.6422	**21.1562**	78	25	56

The objective measures of 3-D FDWT with semisoft thresholding scheme with optimal thresholds values are compared in table (6) that describes the RMSE, SNR and PSNR of different color AVI videos types (*'Xylophone', 'Mosaicking',' Scenevideoclip' ,'Shuttle', 'Visionface', 'Traffic', 'Train' ,'Warnsigns' and 'Vipmen'* respectively *)* of the 35th noisy frame for each of them (which is the first frame of the noisy group frames 35th,36th,37th and 38th) with (σ=20). Note that 3-D FDWT results have the best result than of 2-D FDWT.

Table (6): RMSE, SNR and PSNR results with Haar filter using 3-D FDWT.

Noisy frames				Denoising by 3-D FDWT and Semisoft thresholding			
Video name	**RMSE**	**SNR dB**	**PSNR dB**	**RMSE**	**SNR dB**	**PSNR dB**	**Optimal threshold**
Xylophone	20.0276	16.0530	21.6096	10.6511	21.4497	27.1188	45
Mosaicking	19.9967	17.7307	21.0426	12.0194	22.1014	25.4991	44
Scenevideoclip	20.0535	20.0473	22.0768	15.1047	22.4731	24.5487	37
Shuttle	20.0770	18.3833	21.3812	9.5195	24.7979	27.8633	50
Visionface	20.0770	16.0849	22.0426	12.5810	20.0403	26.1047	40
Traffic	20.0283	16.4983	21.3160	11.9189	20.9103	25.8466	42
Train	19.9593	15.9440	21.2887	11.9355	20.3406	25.8065	42
Warnsigns	19.9632	17.6894	21.0121	11.7949	22.2185	25.6334	45
Vipmen	20.0818	15.7665	22.0197	10.7766	21.0508	27.4303	44

10. Conclusions and Discussions

Three dimensional Fast Discrete Wavelet Transform (FDWT) play an important role in video denoising applications due to the additional dimension (z) of transformation through dealing with temporal correlations between video frames. Some important conclusions will be presented as follows: The results of work are performed using different color AVI video type corrupted by Additive Gaussian White Noise. The type of denoising process is done by using three types of the thresholds (hard, soft and semisoft). Semisoft threshold gives the best result compared with hard and soft threshold for example for example in 3-D DDWT the noisy 20th frame of '*Xylophone*' AVI color video with RMSE equal to (25.0963) becomes (8.7337) in hard threshold became (11.6111) in soft threshold and (8.5132) in semisoft threshold.

Comparing the 2-D FDWT and 3-D FDWT results give an idea that 3-D FDWT eliminates the noise from video better than using 2-D FDWT, for example in the noisy 20th frame of '*Xylophone*' AVI color video with RMSE equal to (25.0963) becomes (17.0908) in 2-D FDWT and (11.0397) in 3-D FDWT. On different color video tested, one can show that 3-D FDWT does better than 2-D FDWT in eliminating video noises.

In 2-D FDWT the proposed 2-D MSDWTM with doubly local wiener filter gives better results in subjective and objective tests than the original 2-D FDWT. Also, the proposed 2-D MSDWTM with one local and one global wiener filter gives better results than the proposed 2-D MSDWTM with doubly local wiener filter and the original 2-D FDWT for example in the noisy 20th frame of '*Xylophone*' AVI color video with RMSE equal to (25.0963) becomes (17.0908) in 2-D FDWT and (12.1897) in 2-D MSDWTM with doubly local wiener filter and (12.0029) in 2-D MSDWTM with one local and one global wiener filter.

In 3-D FDWT the proposed 3-D MSDWTM with doubly local wiener filter achieve the better results than 3-D FDWT and the proposed 3-D MSDWTM with one local and one global wiener filter gives the better results than the proposed 3-D MSDWTM with doubly local wiener filter and the original 3-D FDWT for example in the noisy 20th frame of '*Xylophone*' AVI color video with RMSE equal to (25.0963) becomes (11.0397) in 3-D FDWT and (9.9882) in 3-D MSDWTM with doubly local wiener filter and (9.7218) in 3-D MSDWTM with one local and one global wiener filter.

11. References

1. Dai J., Oscar ,C. Au., Zou F., and Pang C.," Generalized Multihypothesis Motion Compensated Filter for Grayscale and Color Video Denoising ", Signal Processing, Vol. 93, PP 70–85, 2013.

2. Xue G.," Temporal Denoising of High Resolution Video", M.Sc. Thesis, Univ. of McMaster, Electrical and Computer Eng. Dep. 2009.

3. Bahich M., Bailich M., Imloul A., Afifi M., and Barj E.," A Comparative Study of One and Two-Dimensional Wavelet-Based Techniques for Noisy Fringe Batterns Analysis", Optics Communications, Vol. 290, PP 43–48, 2013.
4. Om H., and Biswas M.," An Improved Image Denoising Method Based on Wavelet Thresholding ", Journal of Signal and Information Processing, Vol. 3, PP 109-116, 2012.

5. Al-Taai H. N., " Computationally Efficient Wavelet Based Algorithms for Optical Flow Estimation ", Ph.D. Thesis, Univ. of Technology, Electrical and electronic engineering,Dep., Oct.2005.

6. Bijalwan A., Goyal A., and Sethi N., " Wavelet Transform Based Image Denoise Using Threshold Approaches ", International Journal of Engineering and Advanced Technology,Vol.1, No. 5, ISSN 2249 – 8958, PP. 218-221, June, 2012 .

7. Umbangh S. E., "Computer Vision and Image Processing", A practical approach using CVIP tools, Prentice Hall, Inc., Upper Saddle River, NJ 07458 (U.S.A.), 1998.

8. Al-Saraf T.O.K.," Fingerprint Recognition Using 3D Wavelet and 3D Multiwavelet With Neural Network", M.Sc. Thesis, Univ. of Sulayimani, Computer Science,Dep., Dec.2006.

9. Eristi H., " Fault Diagnosis System for Series Compensated Transmission Line Based on Wavelet Transform and Adaptive Neuro-Fuzzy Inference System ", Measurement,Vol.46, PP. 393-401 , 2013.
10. AbdulWahab M.S., " 3D Wavelet-Based Optical Flow Estimation ", Eng. & Technology, Vol.25, No.2, PP. 299-311 , 2007 .
11. Geng P., Xianbin L. Wanhai Y., Shiqiang,Y.,and Jianhu L., " A Video Denoising Method Based on Grouping the Similar Blocks and Surfacelet", Research Journal of Applied Sciences, Engineering and Technology, ISSN: 2040-7467Vol. 3 No.,10 PP. 1182-1187 , 2011 .
12. Akshay N., B.Satish, and B.L.Raju " Implementation Of 3D DWT With 5/3 LeGall Filter For Image Processing ", International Journal on Computer Science and Engineering, ISSN : 0975-3397 Vol. 4 No.5, PP. 729- 734 May, 2012 .
13. Goswami J. C., and Chan A. K., "Fundamentals of Wavelets Theory, Algorithms, and Applications", John Willy and Sons, 1999.
14. Abdulmunim M. E. A., " Color Image Denoising Using Discrete Multiwavelet Transform", Ph.D. Thesis, Univ. of Technology, Computer Science and Information Sys. Dep., 2004.
15. Jakiwer M.J.,"Quantitative Analysis of Denoising SAR Images ", M.Sc. Thesis, Univ. of Technology, Computer Science,Dep., Dec.2003.

رفع التشويش من الفيديوات الملونة بتطوير عدة تقنيات نقل

أ.م.د. مثيل عمادالدين عبدالمنعم* رباب عباس فرحان**

المستخلص

اكثر الطرق المقترحة لتقليل الضوضاء مطبقة على الصور الثابتة في حين ان عدد قليل تم اقتراحها لتقليل الضوضاء في الفيديو وحتى اقل عندما يتعلق الامر بالفيديو الملون.

ان التحويل الثلاثي الأبعاد هو وسيلة جيدة لحل مشكلة معالجة الفيديو مثل تقليل ضوضاء الفيديو لانه يتعامل مع الارتباطات المكانية والزمانية بين اطارات الفيديو. انها تميل للحد من الضوضاء في متواليات الفيديو مقارنة مع التحول ثنائي الابعاد الذي يتعامل مع المعلومات المكانية فقط.

هذا البحث يهدف الا اقتراح طرق لرفع الضوضاء والمسماة (MSDWTM) . هذه الطريقة طبقت على الـ FDWT ذو البعدين والثلاثة ابعاد واعطت نتائج جيدة مقارنة مع الطرق الأصلية بدون التبديل وباستخدام قاعدة بيانات من الفيديوات الملونة. وعندما كان الـ RMSE مساويا الى (25.0963) فقد تم تخفيضه بطرق FDWT الثنائية والثلاثية الأبعاد الى (7.3511) و (7.1080).

*قسم علوم الحاسوب/الجامعة التكنولوجية
** قسم هندسة الأنتاج والمعادن/الجامعة التكنولوجية